Carbamates with Differential Mechanism of Inhibition Toward Acetylcholinesterase and Butyrylcholinesterase

Sultan Darvesh,*,[†,‡,§] Katherine V. Darvesh,[§] Robert S. McDonald,[§] Diane Mataija,[§] Ryan Walsh,[‡] Sam Mothana,[§] Oksana Lockridge,[∥] and Earl Martin[§]

Department of Medicine (Neurology), Dalhousie University, Halifax, Nova Scotia, Canada, Department of Anatomy and Neurobiology, Dalhousie University, Halifax, Nova Scotia, Canada, Department of Chemistry, Mount Saint Vincent University, Halifax, Nova Scotia, Canada, Eppley Institute, University of Nebraska Medical Center, Omaha, Nebraska

Received February 27, 2008

Most carbamates are pseudoirreversible inhibitors of cholinesterases. Phenothiazine carbamates exhibit this inhibition of acetylcholinesterase but produce reversible inhibition of butyrylcholinesterase, suggesting that they do not form a covalent bond with the catalytic serine. This atypical inhibition is attributable to $\pi-\pi$ interaction of the phenothiazine moiety with F329 and Y332 in butyrylcholinesterase. These residues are in a helical segment, referred to here as the E-helix because it contains E325 of the catalytic triad. The involvement of the E-helix in phenothiazine carbamate reversible inhibition of butyrylcholinesterase is confirmed using mutants of this enzyme at A328, F329, or Y332 that show typical pseudoirreversible inhibition. Thus, in addition to various domains of the butyrylcholinesterase active site gorge, such as the peripheral anionic site and the π-cationic site of the Ω-loop, the E-helix represents a domain that could be exploited for development of specific inhibitors to treat dementias.

Introduction

Acetylcholinesterase (AChE, EC 3.1.1.7) and butyrylcholinesterase (BuChE, EC 3.1.1.8) are serine hydrolases that catalyze the hydrolysis of acetylcholine, thus regulating cholinergic neurotransmission.[1–3] In disorders such as Alzheimer's disease (AD),[a] where there is diminished cholinergic activity, treatment with cholinesterase inhibitors has been shown to be beneficial.[4] A number of different types of cholinesterase inhibitors are known and have been found to affect these enzymes in a variety of ways. Compounds like donepezil and galantamine produce reversible inhibition where the inhibitor interferes with substrate hydrolysis by transiently interacting with the enzyme, without forming a covalent bond.[5–8] On the other hand, organophosphates (such as diisopropylfluorophosphate) inhibit the same enzymes irreversibly by forming a strong covalent bond with the serine of the catalytic triad.[1,8] Carbamates tend to fall between these extremes in that they carbamylate the catalytic serine, but the inhibition is "pseudoirreversible" or "slowly reversible" because the acylated intermediate is slowly hydrolyzed to reactivate the enzyme.[8]

Cholinesterase inhibitors, including carbamates, have gained much attention since they have been successfully used in the treatment of a number of diseases involving cholinergic dysfunction. In fact, a carbamate, the naturally occurring physostigmine, was the first clinically employed cholinesterase inhibitor, used by Laqueur over a century ago to treat glaucoma.[8] Since then, many carbamates have been synthesized and have

been used to treat other disorders of cholinergic neurotransmission.[8–12] Furthermore, selection of unique carbamate molecular properties has proved valuable in targeting specific disorders. Thus, a carbamate such as pyridostigmine is used to treat motor weakness in myasthenia gravis because this molecule, because of its polar nature, does not readily cross the blood–brain barrier and predominantly targets cholinesterases in the periphery.[8] Hydrophobic carbamates, such as rivastigmine[9] and phenserine,[12] readily cross the blood–brain barrier to inhibit cholinesterases in the central nervous system, leading to improved cognition in dementias.

Derivatives of phenothiazine are known to inhibit cholinesterases, especially BuChE,[13–15] and one BuChE-specific phenothiazine inhibitor, ethopropazine, has been shown to improve cognitive function.[16] To explore further structure–activity relationships for inhibition of cholinesterases by phenothiazines, a number of phenothiazine carbamate derivatives were synthesized and evaluated for their inhibitory properties toward human cholinesterases. Although carbamates are generally known to inhibit AChE and BuChE by a common mechanism involving covalent bond formation at the active site serine (Figure 1), phenothiazine carbamates show reversible inhibition of BuChE while exhibiting the more common pseudoirreversible inhibition of AChE. It has been suggested that phenothiazine derivatives inhibit BuChE by binding to F329 and Y332 (Figure 1) near the mouth of the active site gorge.[15,17] Such an interaction with the corresponding F338 and Y341 in AChE is not possible because of steric interference by Y337[17] (Figure 1). We therefore hypothesized that phenothiazine carbamates exhibited reversible inhibition of BuChE because of the interaction between F329 and Y332 of BuChE with the benzene rings of the phenothiazine tricycle. This would preclude the carbamate from reaching, and carbamylating, S198 of the BuChE catalytic triad. To test this hypothesis, a number of BuChE mutants were examined that had alterations in the helical segment from E325 of the catalytic triad to Y332 at the mouth of the active site gorge. For ease of reference, this helical portion of the active site gorge will be referred to as the E-helix because it contains a component of

* To whom correspondence should be addressed. Phone: 902-473-2490. Fax: 902-473-7133. E-mail: sultan.darvesh@dal.ca. Address: Room 1308, Camp Hill Veterans' Memorial Building 1, 5955 Veterans' Memorial Lane, Halifax, Nova Scotia, Canada, B3H 2E1.

† Department of Medicine (Neurology), Dalhousie University.

‡ Department of Anatomy and Neurobiology, Dalhousie University.

§ Department of Chemistry, Mount Saint Vincent University.

∥ Eppley Institute, University of Nebraska Medical Center.

[a] Abbreviations: AChE, acetylcholinesterase; BuChE, butyrylcholinesterase; AD, Alzheimer's disease; DTNB, 5,5′-dithiobis (2-nitrobenzoic acid); MMFF, Merck molecular force field; SMILES, simplified molecular input line entry system.
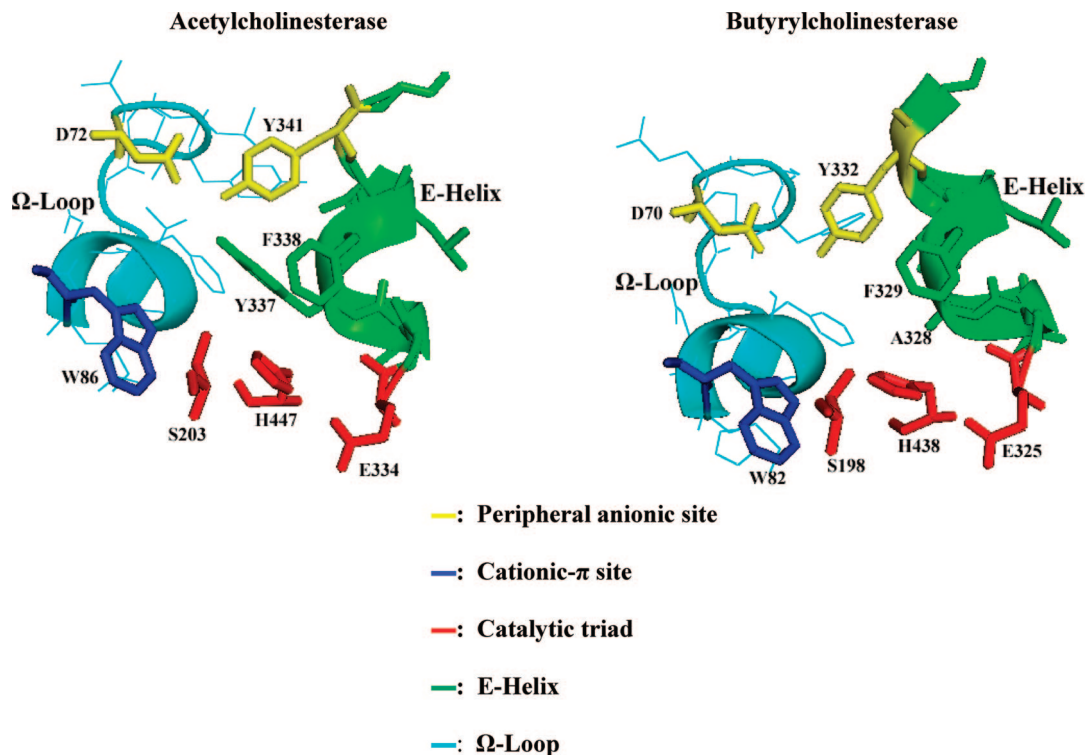
Figure 1. Active site regions of human acetylcholinesterase and human butyrylcholinesterase. The figure was generated using crystal structure of acetylcholinesterase[5] (PDB ID: 1EVE) and butyrylcholinesterase[33] (PDB ID: 1POI) obtained from the protein databank[34] and using PyMol.[35]

the enzyme catalytic triad, E325 in BuChE and E334 in AChE (Figure 1). Changes in amino acid residues in the E-helix in BuChE are observed to alter the reversible inhibition by phenothiazine carbamates, seen for wild-type enzyme, to pseudoirreversible inhibition of the mutant enzyme species. Certain domains of the active site gorge, such as the peripheral anionic site and the π-cationic site, that are part of the Ω-loop,[18,19] have been shown to be involved in reversible inhibitor binding.[5,6] Evidence presented here suggests that an additional domain, the E-helix region containing F329 and Y332, represents a domain that could be exploited as a target for development of specific cholinesterase inhibitors to treat dementias such as AD.

Results and Discussion

A total of 29 carbamate derivatives of phenothiazine were synthesized according to the reaction scheme depicted in Figure 2. Of these, 10 compounds (**1**,[20] **2**,[21] **4**,[21] **6**,[21] **8**,[20,22] **9**,[20] **10**,[22] **11**,[20] **13**,[23] and **14**[24]) have been synthesized previously. The structures of all 29 compounds are shown in Tables 1 and 2. All the derivatives were *N*-(10)-carbamates with variously substituted alkyl-, aminoalkyl-, and aryl-side groups. Each carbamate derivative was examined for its ability to inhibit human AChE and BuChE.

Synthetic Chemistry. The alkyl and aryl phenothiazine carbamates were prepared by refluxing, in dichloromethane, phenothiazine-10-carbonyl chloride with an excess of the alcohol or phenol and an equivalent amount of triethylamine to neutralize the generated HCl. In the preparation of the alkylamino carbamates, triethylamine was not used. Because the alkyl and aryl carbamates could not be cleanly separated from remaining phenothiazine-10-carbonyl chloride by thin layer chromatography or column chromatography, any unreacted carbonyl chloride was reacted with propylamine to form the corresponding propyl urea derivative of phenothiazine, which
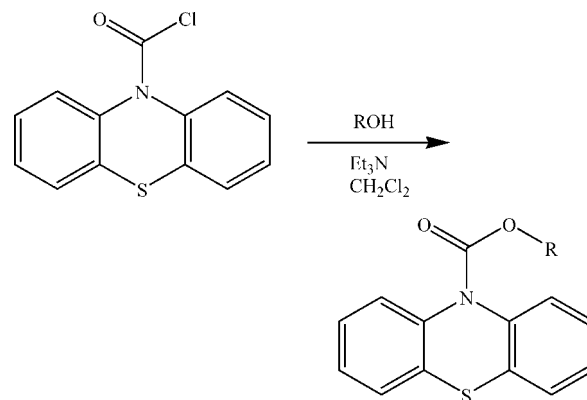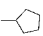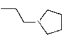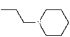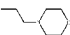

Figure 2. General reaction scheme. Scheme for synthesis of *N*-(10)-substituted phenothiazine carbamate derivatives. The R groups are shown in Tables 1 and 2.

could be readily separated from the desired phenothiazine carbamates. After workup, carbamate purification was achieved by silica gel column chromatography and crystallization. The alkylamino phenothiazines were isolated as hydrochloride salts. All purified compounds were homogeneous by thin layer chromatography. HPLC analysis and ^{1}H NMR revealed all synthesized compounds to be more than 98% pure. All compounds were fully characterized by IR, ^{1}H, and ^{13}C NMR spectroscopy, as well as low- and high-resolution (accurate mass) mass spectrometry. Physical data were consistent with the structure (Tables 1 and 2) of each molecule synthesized.

Enzyme Kinetic Studies. All assays were carried out using a modification[25] of the Ellman method[26] as outlined in detail in the Experimental Section. Each phenothiazine carbamate was tested for its ability to effect time-dependent deactivation of AChE and BuChE. This was done by determining the extent of inhibition of AChE or BuChE at time zero (enzyme added to the assay last to initiate the reaction) and preincubation of the

Table 1. Alkyl and Aminoalkyl Phenothiazine Carbamates[a]

	Name	R =	AChE k_a $M^{-1}min^{-1}$ (x 10^3)	BuChE K_i M (x 10^{-6})	Volume $Å^3$	Log P
			Alkyl phenothiazine carbamates			
1.	Methyl	-CH$_3$	0.426 ± 0.037	10.2 ± 2.3	250	3.66
2.	Ethyl	-CH$_2$CH$_3$	0.193 ± 0.022	23.4 ± 5.0	269	4.07
3.	Propyl	-CH$_2$CH$_2$CH$_3$	0.219 ± 0.035	260 ± 27.7	287	4.49
4.	Isopropyl	-CH(CH$_3$)$_2$	1.8 ± 0.07	18.1 ± 3.5	287	4.45
5.	n-Butyl	-CH$_2$CH$_2$CH$_2$CH$_4$	0.135 ± 0.064	13.4 ± 1.3	305	4.97
6.	t-Butyl	-C(CH$_3$)$_3$	0.219 ± 0.08	4.3 ± 0.9	305	4.86
7.	Cyclopentyl		0.492 ± 0.185	3.19 ± 1.0	312	5.01
			Alkylamino phenothiazine carbamates			
8.	2-(N,N-Dimethylamino)ethyl	-CH$_2$CH$_2$N(CH$_3$)$_2$	0.546 ± 0.082	2.45 ± 0.14	319	3.74
9.	2-(N,N-Diethylamino)ethyl	-CH$_2$CH$_2$N(CH$_2$CH$_3$)$_2$	0.24 ± 0.006	0.61 ± 0.12	356	4.57
10.	3-(N,N-Diethylamino)propyl	-CH$_2$CH$_2$CH$_2$N(CH$_2$CH$_3$)$_2$	0.21 ± 0.03	0.74 ± 0.26	374	5.02
11.	2-Pyrrolidinylethyl		46.0 ± 4.1	0.65 ± 0.08	344	4.27
12.	2-Piperidinylethyl		3.0 ± 0.9	3.2 ± 1.8	361	4.72
13.	2-(4-Morpholino)ethyl		0.12 ± 0.021	2.4 ± 0.97	352	3.47

[a] k_a values for inhibition by rivastigmine: AChE = 1.13×10^3 M^{-1} min^{-1}; BuChE = 129×10^3 M^{-1} min^{-1}. K_i values for inhibition by donepezil: AChE = 0.024×10^{-6} M; BuChE = 2.21×10^{-6} M. K_i values for inhibition by galantamine: AChE = 0.52×10^{-6} M; BuChE = 2.09×10^{-6} M.[7]

enzyme with the inhibitor at regular time intervals for up to 30 min. None of the derivatives showed pseudoirreversible inhibition of purified human plasma wild-type BuChE, as evidenced by the absence of additional loss of enzyme activity after preincubation of enzyme with inhibitor. Conversely, all the phenothiazine carbamates described here showed time-dependent deactivation of purified recombinant human AChE (Tables 1 and 2) because there was an increase in the extent of inhibition of this enzyme with increase in time of preincubation of the enzyme and inhibitor.

The second-order rate constants (k_a values) for AChE deactivation were obtained by comparing enzyme activity at time zero (enzyme added to the assay mixture last) to the activity obtained after preincubation of enzyme with a carbamate for periods of up to 30 min. The k_a value for each carbamate was determined from this data by methods described earlier.[7,27,28] An example of such a determination is shown in Figure 3, where k_a is obtained as the slope of the straight line (see Experimental Section for details).

Human wild-type BuChE, which showed no pseudoirreversible inhibition by phenothiazine carbamates, was tested for immediate reversible inhibition by comparing assay in the absence of the inhibitor, to a reaction mixture containing various amounts of inhibitor. This gave an enzyme activity−inhibitor concentration profile from which could be selected inhibitor concentrations suitable for kinetic studies. Inhibition constants for BuChE (K_i values, Tables 1 and 2) were obtained from Lineweaver−Burk double reciprocal plots, an example of which is shown in Figure 4 (see Experimental Section for details).

Molecular Computational Studies. Computational methods were used to examine molecular characteristics that could influence cholinesterase inhibition by phenothiazine carbamates. One of these parameters was total molecular volume, derived from molecular mechanics calculations of the minimum energy
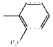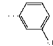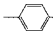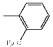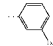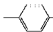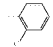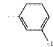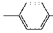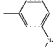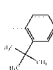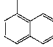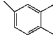
conformation for each derivative. Molecular mechanics calculations were carried out using Spartan '06[29] in which the Merck molecular force field (MMFF) was employed, with the keyword "equilibrium conformer", so that the most stable conformer would be selected.

Also calculated by molecular mechanics for each derivative was the "butterfly angle" for the phenothiazine tricyclic ring system. The butterfly angle refers to the angle between the two planes defined by the benzene rings of the phenothiazine tricycle.[14] For all compounds, this was consistently 146 ± 0.1°. The butterfly conformation of the phenothiazine tricycle provides an appropriate shape for $\pi-\pi$ stacking of the benzene rings of this moiety with F329 and Y332 (Figure 1) within the BuChE active site gorge as suggested earlier.[14,15,17]

For each derivative, log P value was calculated in order to predict the ability of the derivative to cross the blood−brain barrier.[15,30] Experimentally, the log P value of a particular molecule is determined by partitioning the molecule between polar water and nonpolar n-octanol as competing solvents. However, when solubility and detection limits do not permit experimental determination, as with phenothiazines, log P values can be calculated via programs such as the ALOGPS v. 2.0, which is available on line.[30] This method compares the structure of the molecule being considered to a large database of log P values for known molecules. The larger the value of log P, the greater the probability that the molecule will be able to cross the blood−brain barrier. Although very high log P values can be associated with decreased aqueous solubility and potentially limited absorption, all of the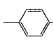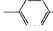 phenothiazine derivatives examined here had calculated log P values of 3 to less than 7 (Tables 1 and 2). These values are comparable to those calculated earlier for drugs currently used to treat AD.[15]

Structure−Activity Relationships. Most known carbamates deactivate cholinesterases by time-dependent covalent bond

Table 2. Aryl Phenothiazine Carbamates

	Name	R =	AChE k_a M^{-1}min^{-1} (x 10^3)	BuChE K_i M (x 10^{-6})	Volume Å^3	Log P
14.	Phenyl		46.0 ± 12.0	0.57 ± 0.1	316	5.28
15.	2-Methylphenyl		547.0 ± 42.4	0.39 ± 0.14	335	5.52
16.	3-Methylphenyl		7.49 ± 1.3	1.69 ± 0.62	335	5.59`
17.	4-Methylphenyl		92.6 ± 6.9	2.85 ± 1.18	335	5.67
18.	2-Methoxyphenyl		5.99 ± 0.17	0.34 ± 0.02	343	4.93
19.	3-Methoxyphenyl		89.4 ± 8.9	0.71 ± 0.12	344	5.19
20.	4-Methoxyphenyl		1.42 ± 0.18	2.26 ± 0.39	344	5.17
21.	2-Chlorophenyl		18.7 ± 4.67	45.4 ± 15.9	330	5.63
22.	3-Chlorophenyl carbamate		3.21 ± 0.97	0.57 ± 0.17	330	5.66
23.	4-Chlorophenyl carbamate		7.25 ± 1.59	10.5 ± 2.1	326	5.67
24.	3-(N,N-dimethylamino)phenyl		19,200.0 ± 1.201	1.91 ± 0.14	366	5.38
25.	2-t-Butylphenyl		0.011 ± 0.004	0.12 ± 0.07	388	6.71
26.	4-t-Butylphenyl		0.63 ± 0.07	[a]No inhibition	389	6.81
27.	4-Biphenyl		910.0 ± 326.9	[b]No inhibition	400	6.90
28.	1-Naphthyl		1650.0 ± 51.3	0.036 ± 0.01	367	5.73
29.	2-Naphthyl		11.2 ± 0.96	0.12 ± 0.008	367	6.40

[a] No inhibition detected up to [I] = 7.33 × 10^{-5} M, the solubility limit. [b] No inhibition detected up to [I] = 2.36 × 10^{-5} M, the solubility limit.

formation (carbamylation) at the active-site serine[1] that prevents substrate hydrolysis (Figure 5A,B,C). The resulting carbamylated serine residue subsequently undergoes hydrolysis to regenerate the active enzyme (Figure 5D,E,F), leading to the designation of such compounds as pseudoirreversible inhibitors. Typically, when such a compound inhibits cholinesterases, the mechanism of inhibition is the same for both AChE and BuChE because they both have the same catalytic triad composed of the nucleophilic serine, histidine, and glutamate (Figure 1). However, phenothiazine carbamates did not exhibit the same type of inhibition for the two cholinesterases. All did show the expected pseudoirreversible carbamylation of AChE (Tables 1 and 2) but, in stark contrast, BuChE inhibition was found to be the reversible type, indicating the absence of covalent bond formation with this enzyme (Tables 1 and 2).

Inhibition of Acetylcholinesterase by Phenothiazine Carbamates. The carbamate-induced deactivation of AChE was evaluated by measuring the second-order rate constant for loss of enzyme activity (k_a value).[27,28] Most alkyl phenothiazine carbamates (Table 1) exhibited relatively small k_a values, ranging from 135 to 492 M^{-1}min^{-1} and indicating low potency as AChE inhibitors. The single exception was the isopropyl derivative (**4**), which had a k_a value of 1800 M^{-1} min^{-1}, comparable to that of rivastigmine (1130 M^{-1} min^{-1}).[25]

The molecular volumes of the alkyl phenothiazine derivatives (Table 1) were comparable to the estimated active site gorge volume for AChE (302 Å^3)[17] so that size alone would not make these carbamates poor inhibitors of AChE. However, it is not unexpected that alkyl carbamates should be less potent pseudoirreversible inhibitors of AChE than rivastigmine because the latter carbamate generates a resonance-stabilized phenoxide anion as a leaving group in the enzyme carbamylation step (Figure 5C). In contrast, the alkyl carbamates must produce a highly basic alkoxide ion in the same step. This type of unfavorable leaving group should also be true for the isopropyl carbamate (**4**), which makes its relatively high inhibitor potency difficult to explain unless the compact nature of the isopropyl substituent facilitates interaction of the carbamate with the aryl-rich gorge of AChE. Such affinity could promote passage of the inhibitor down the gorge to S203 of the catalytic triad. This notion is supported by the observation that other compact alkyl groups (as in **1** and **7**) also show more potent AChE inhibition when compared to most of the alkyl carbamates in Table 1.

Several alkylamino phenothiazine carbamates, specifically **8**, **9**, **10**, and **13** (Table 1), were, like most of the alkyl carbamates, weak inhibitors of AChE. The unstable alkoxide leaving group from carbamylation by these derivatives may again be a dominant factor in the low inhibitor potency. However, within this group of compounds there were also notable exceptions. Compared to rivastigmine, the 2-pyrrolidinylethyl carbamate (**11**) was a 40-fold better inhibitor, while 2-piperidinylethyl derivative (**12**) was roughly 3 times better at inactivating AChE. It is possible that the earlier arguments for delivery of the more potent compact alkyl carbamates (**1**, **4**, and **7**) are also operating
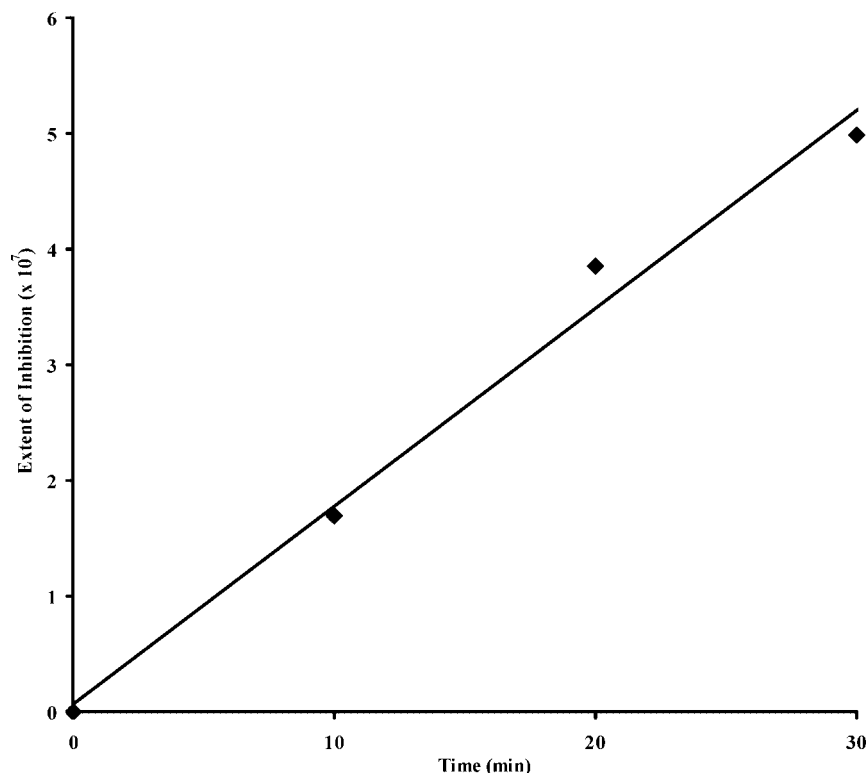
Figure 3. Kinetic plot for inhibition of human acetylcholinesterase by 1-naphthyl phenothiazine carbamate (**28**). The k_a value was calculated by plotting the extent of inhibition {ln (e_o/e_t)/[I]} against time, where e_0 is the enzymatic activity at time zero (without preincubation of enzyme and inhibitor), e_t is the enzymatic activity at time t min of preincubation, and [I] = 5.18×10^{-7} M **28**. The slope of this plot gave the second-order rate constant (k_a value M^{-1} min^{-1}).
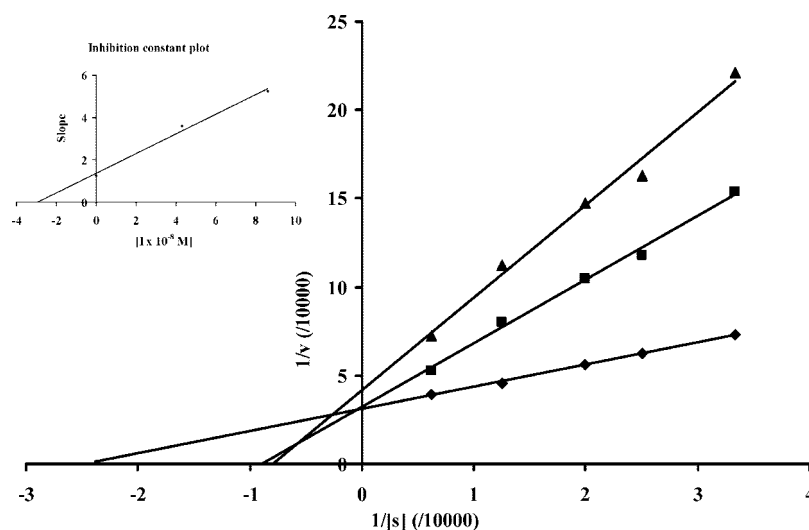
Figure 4. Lineweaver−Burk plot, where the reciprocal of the velocity of the reaction v (M min^{-1}) is plotted against the reciprocal of the substrate concentration s (M), for reversible inhibition of wild-type human butyrylcholinesterase in the absence and presence of 1-naphthyl phenothiazine carbamate (**28**): (▲) no inhibitor; (●) 4.32×10^{-8} M **28**; (■) 8.64×10^{-8} M **28**. Replot of the slopes of the lines versus inhibitor concentration [I] (M) gave the inhibitor constant K_i (M) as the x-intercept (inset).

here with **11** and **12**. In addition, in view of the superior AChE inhibition by **11**, it is possible that the protonated heterocyclic nitrogen atom of the pyrrolidinyl group may be so positioned as to permit favorable π-cationic interaction with W86 of the enzyme (Figure 1), thereby stabilizing the inhibitor for reaction in the active site gorge, as occurs with acetylcholine at this site. Furthermore, in **11**, the presence of a cationic nitrogen may help stabilize the oxyanion leaving group through intramolecular general acid catalysis.

Most aryl phenothiazine carbamates (Table 2) were significantly better at inactivating AChE than rivastigimine. All of these carbamates, including rivastigmine, produce a resonance-stabilized phenoxide anion leaving group in the carbamylation step (Figure 5C). To determine whether electronic effects on the stability of the phenoxide leaving group could be contributing to enhanced potency of phenothiazine carbamates, variously substituted phenyl carbamates were examined (Table 2). There was no clear pattern to suggest predominant electronic effects
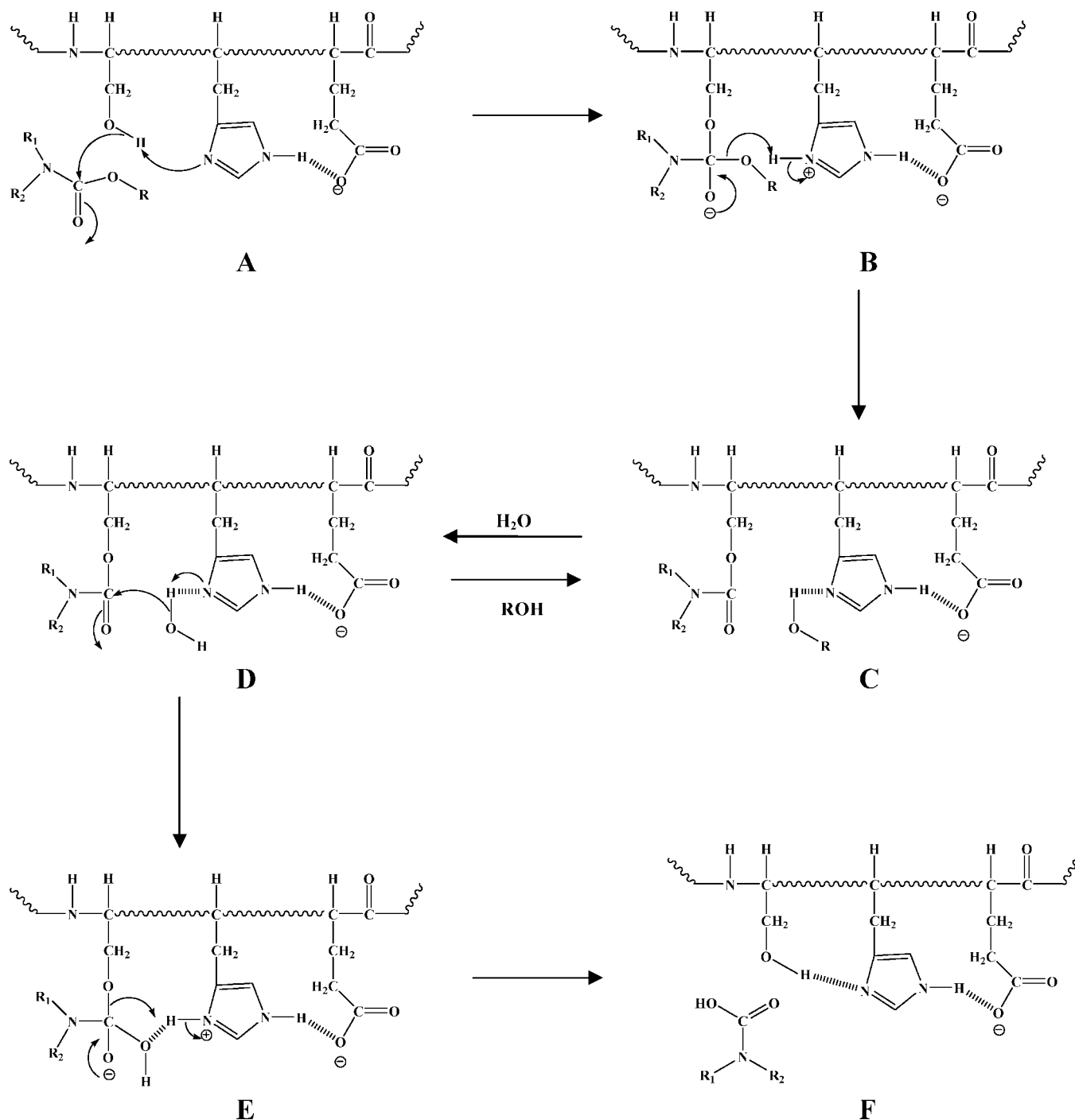
Figure 5. General mechanism of pseudoirreversible cholinesterase inhibition by carbamates. Enzyme deactivation is initiated by nucleophilic attack of the catalytic triad serine oxygen on the carbonyl group of the carbamate.

because identical substituents in the ortho-, meta- or para-positions did not lead to consistent predictable pattern in inhibitor potencies (Table 2). The one possible exception was with the strongly electron-releasing methoxy substituent in compounds **18**, **19**, and **20**. This series exhibited a weakening effect on k_a when this group was in the ortho- (**18**) or para- (**20**) position where electron donation could destabilize the phenoxide leaving group. This is reflected in the low k_a values of **18** and **20** when compared to the meta-derivative (**19**), where the methoxy group tends to be electron-withdrawing, or to the unsubstituted phenyl carbamate (**14**).

Steric hindrance within the AChE gorge produced by the bulky 2-t-butyl derivative (**25**) helps explain this carbamate

being roughly 60-fold less potent than the para-counterpart (**26**). Steric effects may also make 2-naphthyl (**29**) some 150-fold less potent than the corresponding 1-naphthyl derivative (**28**) that presents a much different conformation because of its point of attachment to the phenothiazine, as was seen with comparable amide derivatives.[15]

Of all the synthesized phenothiazine carbamates, the best inhibitor of AChE was 3-(N,N-dimethylamino)phenyl (**24**) (k_a = 19.2 × 10^6 M^{-1} min^{-1}). The potency of this derivative is not readily explained on electronic or steric grounds. It is possible that, for this compound (**24**), the side group nitrogen or phenyl ring may enhance the binding of the compound to AChE, possibly with W86. Such interaction could greatly

improve the affinity of the enzyme for this molecule and facilitate rapid carbamylation of S203 (Figure 1).

One of the most striking features of the aryl phenothiazine carbamates is the very high inhibitor potency for AChE seen for derivatives such as **24**, **27**, and **28** in spite of the large total molecular volume of these compounds (Table 2) relative to the AChE gorge volume (302 Å^3).[17] This implies that only the portion of the molecule containing the carbamate moiety need be delivered to S203 for covalent bond formation to occur.

Inhibition of Wild-Type Butyrylcholinesterase by Phenothiazine Carbamates. All the phenothiazine carbamate derivatives examined inhibited BuChE, except **26** and **27**, the latter compounds being subject to solubility limitations. Of the 27 derivatives that inhibited BuChE, 19 were comparable to, or better than, donepezil or galantamine in their ability to inhibit this enzyme (Tables 1 and 2). In all cases where BuChE inhibition by phenothiazine carbamates occurred, the type of inhibition was reversible, that is, no time-dependent deactivation of the enzyme was observed. The absence of the usual pseudoirreversible effect, generally characteristic of carbamates, can be attributed to favorable $\pi-\pi$ interaction between the phenothiazine tricycle and aromatic amino acid residues F329 and Y332 above the catalytic triad in the BuChE active site gorge.[15,17]

All seven alkyl phenothiazine carbamates were poor inhibitors compared with either donepezil or galantamine (Table 1). This may be because these alkyl side groups are small and, despite interaction of the phenothiazine moiety with the enzyme, these side groups may have limited ability to block substrate access to the catalytic triad. In contrast, the six aminoalkyl phenothiazine carbamates were comparable or better inhibitors of BuChE relative to donepezil and galantamine (Table 1). This may reflect additional interaction of the protonated nitrogen atom in these side groups with the enzyme. For example, the nitrogen cation of the derivative could interact with the W82 via π-cationic association to provide an additional enzyme-inhibitor ligand.

Of the 14 aromatic phenothiazine carbamates that inhibited BuChE, 12 were comparable to, or superior to, donepezil or galantamine as BuChE inhibitors (Table 2). In general, substitution in the aromatic side group did not have a significant effect on the extent of inhibition. This suggests that electronic effects in the side group do not significantly influence the ability of the phenothiazine moiety to bind to the enzyme. However, the planar nature of the aryl side groups in these derivatives may constitute a major factor in blocking substrate access to the catalytic triad, once the phenothiazine tricycle is bound to the enzyme. For example, the 1-naphthyl derivative (**28**), with a fused bicyclic ring system and larger volume, is roughly a 16-fold more potent inhibitor of BuChE than the phenyl carbamate (**14**).

The putative $\pi-\pi$ interaction between the phenothiazine moiety and the two aromatic residues, F329 and Y332,[17] in BuChE must be highly favored because there is little indication that phenothiazine carbamates reach the bottom of the BuChE active site gorge to react with S198. One factor that may favor the BuChE-phenothiazine $\pi-\pi$ interaction is the "butterfly" shape of the phenothiazine tricycle that facilitates $\pi-\pi$ stacking of the aromatic rings of the tricycle with F329 and Y332 in the gorge.[15] For all of the carbamates reported here, the "butterfly angle" was found to be virtually the same (146.0 ± 0.1°), permitting optimum interaction of the two aromatic rings of phenothiazine with the side chain rings of F329 and Y332 in the BuChE gorge (Figure 6). Unlike the prominent 4-hydroxyphenyl side chain of Y337 in AChE (Figure 1), that interferes
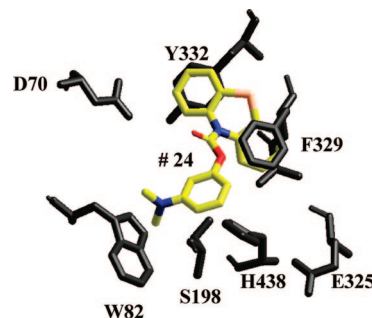

Figure 6. Simulated binding of 3-(*N,N*-dimethyl aminophenyl) phenothiazine carbamate (**24**) to wild-type butyrylcholinesterase through F329 and Y332 on the E-helical segment and utilizing the "butterfly" conformation of the benzene rings of the phenothiazine tricycle to effect $\pi-\pi$ stacking. The figure was generated using HyperChem program,[32] and the crystal structure coordinates of BuChE[33] (PDB ID: 1POI) were downloaded from the protein databank.[34]

with phenothiazine binding,[17] the comparable A328 in BuChE is small and does not interfere with the $\pi-\pi$ overlap of the aromatic rings of enzyme and inhibitor (Figure 6). The reversible inhibition of BuChE by phenothiazine carbamates appears, therefore, to involve a common transient interaction of the phenothiazine moiety with F329 and Y332, and the potency of inhibition can often be attributed to the size of the substituent projecting into the gorge. In addition to blocking substrate, the binding of these phenothiazines to F329 and Y332, these residues being part of the helical polypeptide segment containing E325 of the catalytic triad (E-helix, Figure 1), could result in conformational changes in the triad that, of themselves, could have a negative impact on substrate hydrolysis.

Inhibition of Butyrylcholinesterase Mutants. The selective inhibition of human BuChE by phenothiazine derivatives[15,17] has been ascribed, at least in part, to the interaction between the two aromatic rings of the phenothiazine moiety of these compounds with two aromatic amino acid residues of the enzyme, F329 and Y332 (Figure 6), in the helical segment of the enzyme that contains E325 (E-helix, Figure 1). In fact, this $\pi-\pi$ interaction near the top of the gorge appears to be so influential in the present study of phenothiazine carbamates that it consistently prevents the typical pseudoirreversible reaction between these carbamates and BuChE (Tables 1 and 2). The same $\pi-\pi$ interaction is prevented in AChE because of interference from Y337 that replaces A328 of BuChE (Figure 1), fostering the typical carbamylation of this enzyme. It was therefore hypothesized that altering critical residues in the BuChE active site gorge could alter the type of inhibition produced in BuChE by phenothiazine carbamates. That is, appropriate BuChE mutations at positions 328, 329, and 332 on the E-helix should have a profound effect on the type of observed BuChE inhibition, reversible becoming pseudoirreversible. To test this hypothesis, the carbamate derivative 3-(*N,N*-dimethylamino phenyl) carbamate (**24**), was compared for inhibition of wild-type human BuChE and several site-directed recombinant BuChE mutants, affected in the 328-332 region[31] of the enzyme. This carbamate (**24**) was chosen because, of all the phenothiazine carbamates, it was the most potent pseudoirreversible inhibitor of AChE and a rather poor reversible inhibitor of BuChE ($K_i = 1.91 \times 10^{-6}$ M). Wild-type BuChE showed no time-dependent deactivation but displayed typical reversible inhibition with **24** (see Table 2), where full inhibition is instantaneous and is not altered by preincubation of inhibitor and enzyme. On the other hand, recombinant BuChE mutants tested (Figure 7) were all found to become
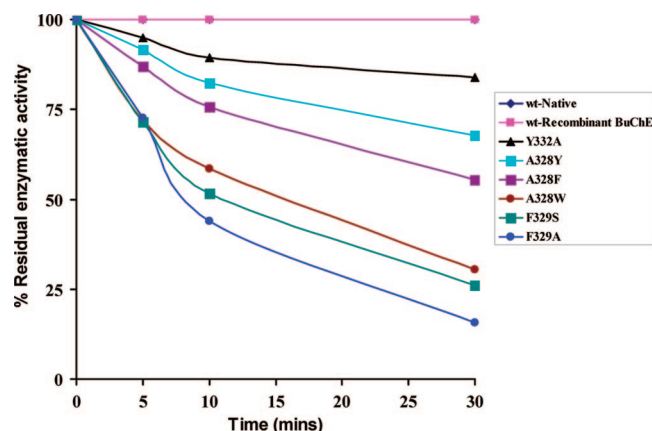
Figure 7. Pseudo-irreversible inhibition of recombinant butyrylcholinesterase mutants by 3-(*N*,*N*-dimethyl aminophenyl) phenothiazine carbamate (**24**) indicated by diminished residual enzyme activity over time. The low concentration of **24** used (4.0×10^{-8} M) produced no instantaneous inhibition of wild-type serum or wild-type recombinant butyrylcholinesterase but showed time-dependent inhibition of mutant butyrylcholinesterases indicating that this carbamate was able to react with S198 of mutant BuChEs but not of the wild-type BuChE.

increasingly deactivated over time, the phenomenon typically observed for carbamylation of the catalytic serine residue. In contrast, neither wild-type native BuChE nor wild-type recombinant BuChE showed time-dependent deactivation by **24** (Figure 7). All six BuChE mutant types depicted in Figure 7 involve residues in the E-helix at positions 328, 329, and 332 (see Figure 1). It was considered that converting F329 or Y332 to alkyl residues should greatly alter the $\pi-\pi$ interaction that is the putative means for reversible inhibition between wild-type BuChE and phenothiazines in general (Figure 6). Likewise, replacing A328 in BuChE with an aromatic amino acid residue should make BuChE more like AChE, which has Y337 in that position (see Figure 1). This should also make the enzyme generally resistant to reversible inhibition by phenothiazine derivatives by disrupting the inhibitor−enzyme $\pi-\pi$ stacking due to new aryl residues at position 328. Figure 7 clearly indicates that such BuChE mutations at 328, 329, or 332 alter the type of inhibition produced by a phenothiazine carbamate, as indicated by increased loss of enzyme activity over time. Of the mutants tested, the most effective change was with F329 converted to the small alkyl side chains of alanine or serine. This inhibition was still some 10-fold less potent than that of the same carbamate (**24**) on AChE (Table 2) but indicated a profound change over the effect of **24** on wild-type native BuChE and wild-type recombinant BuChE, both of which showed no inhibition by **24** at a concentration (4.0×10^{-8} M) that caused time-dependent deactivation of all the mutant enzymes (Figure 7). Replacing A328 with an aryl side chain (A328W, A328F, and A328Y), making BuChE more like AChE in the E-helical segment of the enzyme, had the next most significant effect on BuChE (Figure 7), while the mutant Y332A was the BuChE mutant slowest to be deactivated by **24**. Furthermore, the effect of 4-biphenyl phenothiazine carbamate (**26**) on the same BuChE mutants, as well as two additional mutant enzyme species D70G (the atypical variant) and A539T (the K-variant), also gave predictable results, as summarized in Table 3. That is, a mutation well away from the active site (A539T) showed little tendency to pseudoirreversible inhibition by this phenothiazine carbamate. On the other hand, altering D70, which, like Y332, is considered a component of the BuChE peripheral anionic site, showed similar limited time-dependent deactivation to that observed for Y332A. It seems reasonable

Table 3. Time-Dependent Deactivation of Wild-Type and Mutant Butyrylcholinesterase by 4-Biphenyl Phenothiazine Carbamate (**27**) (2.1×10^{-6} M)

| | %[a] residual enzymatic activity | | | |
butyrylcholinesterase-type	0 min	5 min	10 min	15 min
wild-type native	100	100	100	100
D70G	100	99.5	90	76
A539T	100	99	94	93
Y332A	100	95	87	85
A328Y	100	85	67	63
A328F	100	88	75	59
A328W	100	74	57	35
F329S	100	51	15	11
F329A	100	46	26	12

[a] Obtained from the calculation $[\Delta A/\text{min at time } t \text{ min}/\Delta A/\text{min at time zero}] \times 100$.

to assume that the altered binding of the inhibitor to the BuChE mutant enzyme species exposes S198 to carbamylation.

Conclusions

Carbamate derivatives of phenothiazine are unique in that they generally exhibit only reversible inhibition of BuChE, while producing the common pseudoirreversible inhibition of AChE. The atypical BuChE−phenothiazine carbamate binding is attributable to dominant $\pi-\pi$ interaction between residues F329 and Y332 in BuChE with the phenothiazine aromatic tricycle. This is confirmed with mutations of F329 and Y332 that result in time-dependent deactivation of BuChE.

Interference with similar noncovalent binding in AChE, due to Y337 projecting into the gorge (Figure 1), permits delivery of the phenothiazine carbamate moiety to the bottom of the gorge for reaction with S203. AChE gorge volume is not as restrictive here as it is in reversible inhibition because only the carbamate moiety needs to be delivered to the catalytic triad serine. This is confirmed with BuChE mutants in which A328 is converted to amino acid residues with aryl side chains comparable to Y337 of AChE. These mutations, replacing A328 in BuChE with Y328, F328, or W328, also result in conversion of phenothiazine carbamate inhibition from reversible to pseudoirreversible.

Phenothiazine carbamates with resonance-stabilized aromatic oxyanion leaving groups tend to be the most powerful pseudoirreversible AChE inhibitors.

The lack of covalent bond formation between phenothiazine carbamates and wild-type BuChE implies that such molecules, unlike other carbamates, will not be subject to the typical scavenging by serum BuChE. This, combined with log *P* values favorable for crossing the blood−brain barrier, suggests these hydrophobic phenothiazine carbamates could be developed for treatment of dementia, following appropriate analysis of their effects on other neurotransmitter systems.

In addition to various domains of the active site gorge known to be involved in reversible inhibitor binding, such as peripheral anionic site and the π-cationic site, which are part of the Ω-loop, the E-helix represents a domain that could be exploited as a target for development of specific inhibitors of cholinesterases for treatment of dementias.

Experimental Section

Materials. Purified human plasma butyrylcholinesterase (BuChE, EC 3.1.1.8), purified recombinant wild-type, and mutant BuChEs (Y332A, F329A, A328Y, A328W, A328F, D70G, and A539T) were from Dr. Oksana Lockridge (University of Nebraska Medical Center) (Masson et al., 1997).[31] Purified recombinant human acetylcholinesterase (AChE, EC 3.1.1.7), acetylthiocholine, bu-

tyrylthiocholine, and 5,5′-dithiobis(2-nitrobenzoic acid) (DTNB) were purchased from Sigma (St. Louis, MO). Phenothiazine-10-carbonyl chloride was purchased from Acros Chemicals. The alcohols and phenols were purchased from either Fischer Scientific or Aldrich Chemical Co. Inc. (Milwaukee, Wi).

Organic Synthesis. Synthesis of Aryl-Substituted Carbamates. Typically, a mixture of phenothiazine-10-carbonyl chloride (5.0 mmol), phenol or substituted phenol (20−25 mmol) and triethylamine (5.0 mmol) in CH_2Cl_2 (50 mL) was heated at reflux until analysis by thin layer chromatography revealed no unreacted phenothiazine-10-carbonyl chloride remained or no further change was observed. Reflux periods were typically in the range of 2−10 days. One complication for some of the carbamates was that the R_f values of the products are very similar to that of phenothiazine-10-carbonyl chloride, although sometimes the resulting spots took on a different color after short irradiation periods. As a result, to aid in product purification, propylamine (5.0 mmol) was added to the final reaction mixture to consume any unreacted starting material, which may have been present. The propyl urea thus formed has a much lower R_f value than the carbamates and was readily removed during column chromatography.

For the aryl carbamates, the cooled reaction mixture was poured into a separatory funnel and washed with 5% aqueous sodium hydroxide (2 × 50 mL) to remove unreacted phenolic reactant, followed by water (2 × 50 mL). The organic layer was dried (MgSO_4), filtered, and the solvent removed under reduced pressure.

The crude product was then further purified by column chromatography using silica gel (60−230 mesh) and CH_2Cl_2 as eluent. Fractions containing only the desired product were combined, the solvent removed, and the resulting solid recrystallized using 2:1 petroleum ether:CH_2Cl_2. Activated charcoal was used for the solids that were highly colored. Isolated product yields varied from 31 to 75%; no attempt was made to optimize these yields.

The procedure above did not work well for the 2-*t*-butylphenyl carbamate preparation, presumably due to severe steric effects. In this case, a solution of phenothiazine-10-carbonyl chloride (10 mmol) and 2-*t*-butylphenoxide [15 mmol; prepared from the phenol (20 mmol) and potassium *t*-butoxide (15 mmol)] in tetrahydrofuran (40 mL) was stirred for 21 h at room temperature. After treatment with propylamine (10 mmol) and the addition of water (50 mL), the THF was removed under reduced pressure, CH_2Cl_2 (100 mL) added, and the resulting solution washed with 5% NaOH (2 × 100 mL) followed by water (100 mL). Further isolation and purification followed the procedure above.

Synthesis of Alkylamino Carbamates. The synthetic procedure used for this series was very similar to that outlined above with the elimination of the triethylamine. The products did not move from the baseline using CH_2Cl_2 as eluent for TLC analysis, but this did not compromise monitoring of reaction progress. The solvent system used for purification by column chromatography was 10−20% (by volume) CH_3OH/CH_2Cl_2. Derivatives with the pyrrolidinyl, piperidinyl, and morpholino ring systems were isolated and recrystallized as the free bases. The three acyclic systems produced oils in the free base form; therefore, these were converted to the hydrochloride salts and recrystallized from water. Isolated product yields ranged from 21 to 53%.

Synthesis of Alkyl and Cycloalkyl Carbamates. Reaction of phenothiazine-10-carbonyl chloride with simple alcohols is much slower than that with phenols. For this reason, the alcohol (50 mL) was used as solvent and the reaction of the phenothiazine-10-carbonyl chloride (5 mmol) with triethylamine (5 mmol) was carried out at reflux. Reaction periods were in the range of 7−14 days and, again, because the R_f values of the carbamates were so similar to that of phenothiazine-10-carbonyl chloride, any possible unreacted phenothiazine-10-carbonyl chloride was removed by treatment with propylamine (5 mmol).

Workup involved removal of the excess alcohol under reduced pressure, followed by partitioning of the product between CH_2Cl_2 and water. The organic solution was washed and treated and the product purified as outlined above. Isolated product yields were in the range 16−76%.

A modified procedure was required for the preparation of the *t*-butyl carbamate derivative. In this case, to a solution of phenothiazine-10-carbonyl chloride (10 mmol) in THF (30 mL) was added dropwise a 1.0 M solution of potassium *t*-butoxide in THF (10 mL; 10 mmol) and the resulting solution stirred for 2 days at room temperature. After treatment with propylamine, water (50 mL) was added and the THF removed under reduced pressure. CH_2Cl_2 (50 mL) was added, and the resulting solution was washed and the product isolated and purified as outlined above.

Analysis of Synthesized Compounds. Melting points were determined on a Mel-Temp II apparatus and are uncorrected. Thin layer chromatography was carried out using silica gel sheets with fluorescent indicator (0.20 mm thickness; Macherey-Nagel) and dichloromethane or a dichloromethane/ethyl acetate mixture as developing solvent. Plates were visualized using a short wavelength UV lamp. Infrared spectra were recorded as Nujol mulls between sodium chloride plates on a Nicolet model 205 or a Nicolet Avatar 330 FT-IR spectrometer. Peak positions were reproducible within 1−2 cm^{-1}. Nuclear magnetic resonance spectra were recorded at the Atlantic Region Magnetic Resonance Centre, Dalhousie University, on a Bruker AC-250F operating at 250.1 MHz for proton and 62.9 MHz for carbon or a Bruker AVANCE 500 operating at 500.13 MHz for proton and 125.76 MHz for carbon-13. Chemical shifts are reported in ppm relative to TMS, in CDCl_3 solution. Mass spectra were recorded at Dalhousie University on a CEC 21-110B spectrometer using electron ionization at 70 V and an appropriate source temperature with samples being introduced by means of a heatable port probe. Accurate mass measurements were also made on this machine operated at a mass resolution of 8000 by computer controlled peak matching to appropriate PFK reference ions. Mass measurements were routinely within 3 ppm of the calculated value. The purity of the synthesized compounds was also determined using either an Agilent Technologies 1200 series HPLC system with silica gel column and dichloromethane as the mobile phase or a Waters HPLC system using C18 reverse phase column with methanol as the mobile phase.

Analytical Data. Methyl Carbamate (1). Colorless crystals, mp 116−118 °C (lit. mp 92−93 °C;[20] 118−120 °C[21]). IR (Nujol): 1712, 1330, 1307, 1288, 1263, 1228, 1052, 760 cm^{-1}. ^{1}H NMR (CDCl_3): 3.79 (s, 3H), 7.13−7.20 (m, 2H), 7.25−7.32 (m, 2H), 7.35 (dd, *J* = 7.6 and 1.5 Hz, 2H), 7.54 (dd, *J* = 7.9 and 1.2 Hz, 2H). ^{13}C NMR (CDCl_3): 53.54, 126.46, 126.90, 127.02, 127.58, 132.24, 138.34, 154.27. EI-MS (*m/z*): 257 (M$^+$; base), 200, 199, 198, 154. HR-MS (EI): M$^+$ found, 257.0525; calcd for $C_{14}H_{11}NO_2S$, 257.0510.

Ethyl Carbamate (2). Off-white crystals, mp 102−103.5 °C (lit. mp 116−117 °C[21]). IR (Nujol): 1707, 1322, 1259, 1223, 1044, 1029, 946, 764 cm^{-1}. ^{1}H NMR (CDCl_3): 1.30 (t, *J* = 7.5 Hz, 3H), 4.29 (q, *J* = 7.5 Hz, 2H), 7.15−7.21 (m, 2H), 7.26−7.33 (m, 2H), 7.38 (broad d, *J* ∼ 7.5 Hz, 2H), 7.57 (broad d, *J* ∼ 7.5 Hz, 2H). ^{13}C NMR (CDCl_3): 14.40, 62.68, 126.34, 126.80, 127.07, 127.55, 132.18, 138.44, 153.70. EI-MS (*m/z*): 271 (M$^+$), 200, 199, 198 (base), 197, 167, 166, 154, 140, 127. HR-MS (EI): M$^+$ found, 271.0678; calcd for $C_{15}H_{13}NO_2S$, 271.0667.

Propyl Carbamate (3). Colorless crystals, mp 106.5−107.5 °C. IR: (Nujol): 1708, 1322, 1305, 1288, 1257, 1220, 1066, 909, 755 cm^{-1}. ^{1}H NMR (CDCl_3): 0.90 (t, *J* = 7.4 Hz, 3H), 1.62−1.69 (m, 2H), 4.16 (t, *J* = 6.7 Hz, 2H), 7.14−7.17 (m, 2H), 7.25−7.28 (m, 2H), 7.35 (dd, *J* = 7.7 and 1.3 Hz, 2H), 7.54 (dd, *J* = 8.0 and 0.8 Hz, 2H). ^{13}C NMR (CDCl_3): 10.38, 22.00, 68.13, 126.23, 126.65, 126.97, 127.41, 132.09, 138.33, 153.73. EI-MS (*m/z*): 285 (M$^+$), 199, 198 (base), 171, 167, 166, 154, 140, 127. HRMS (EI): M$^+$ found, 285.0828; calcd for $C_{16}H_{15}NO_2S$, 285.0823.

Isopropyl Carbamate (4). Colorless crystals, mp 137.5−138.5 °C (lit. mp 135 −137 °C[21]). IR (Nujol): 1712, 1319, 1304, 1259, 1228, 1181, 1095, 1038, 767, 752 cm^{-1}. ^{1}H NMR (CDCl_3): 1.26 (d, *J* = 6.3 Hz, 6H), 5.05 (septet, *J* = 6.3 Hz, 1H), 7.13−7.16 (m, 2H), 7.24−7.28 (m, 2H), 7.34 (broad d, *J* ∼ 7.7 Hz, 2H), 7.53 (broad d, *J* ∼ 8.1 Hz, 2H). ^{13}C NMR (CDCl_3): 21.91, 70.62, 126.21, 126.69, 127.10, 127.52, 132.16, 138.56, 153.25. EI-MS (*m/z*): 285

(M$^+$), 199, 198 (base), 170, 167, 166, 153, 140, 126. HR-MS (EI): M$^+$ found, 285.0827; calcd for C$_{16}$H$_{15}$NO$_2$S, 285.0823.

Butyl Carbamate (5). Colorless crystals, mp 51–53 °C. IR (Nujol): 1728, 1322, 1287, 1259, 1220, 1091, 1064, 1033, 728 cm^{-1}. ^{1}H NMR (CDCl$_3$): 0.90 (t, J = 7.4 Hz, 3H), 1.30–1.38 (m, 2H), 1.59–1.65 (m, 2H), 4.20 (t, J = 6.7 Hz, 2H), 7.14–7.17 (m, 2H), 7.25–7.29 (m, 2H), 7.34 (dd, J = 7.8 and 1.2 Hz, 2H), 7.53 (dd, J = 8.1 and 0.8 Hz, 2H). ^{13}C NMR (CDCl$_3$): 13.65, 19.13, 30.70, 66.47, 126.28, 126.70, 127.03, 127.47, 132.16, 138.43, 153.78. EI-MS (*m/z*): 299 (M$^+$; base), 200, 199, 198, 197, 171, 167, 166, 154. HR-MS (EI): M$^+$ found, 299.0984; calcd for C$_{17}$H$_{17}$NO$_2$S, 299.0980.

***t*-Butyl Carbamate (6).** Colorless crystals, mp 116–117 °C (lit. mp 108–110 °C[21]). IR (Nujol): 1709, 1334, 1256, 1232, 1157, 1021, 951, 846, 764 cm^{-1}. ^{1}H NMR (CDCl$_3$): 1.48 (s, 9H), 7.12–7.15 (m, 2H), 7.23–7.27 (m, 2H), 7.33 (dd, J = 7.8 and 1.4 Hz, 2H), 7.52 (dd, J = 8.1 and 1.1 Hz, 2H). ^{13}C NMR (CDCl$_3$): 28.15, 82.05, 126.03, 126.52, 127.19, 127.41, 132.13, 138.72, 152.45. EI-MS (*m/z*): 299 (M$^+$), 244, 243, 200, 199 (base), 198, 167, 166, 154, 140, 128, 127, 57. HR-MS (EI): M$^+$ found, 299.0972; calcd for C$_{17}$H$_{17}$NO$_2$S, 299.0980.

Cyclopentyl Carbamate (7). Colorless crystals, mp 95–97 °C. IR (Nujol): 1708, 1364, 1329, 1288, 1259, 1225, 1168, 1040, 971, 763 cm^{-1}. ^{1}H NMR (CDCl$_3$): 1.5–2.0 (overlapping m, 8H), 5.20–5.27 (m, 1H), 7.11–7.17 (m, 2H), 7.22–7.29 (m, 2H), 7.34 (dd, J = 7.7 and 1.5 Hz, 2H), 7.51 (dd, J = 8.0 and 1.1 Hz, 2H). ^{13}C NMR (CDCl$_3$): 23.49, 32.59, 79.58, 126.11, 126.53, 126.89, 127.36, 131.95, 138.37, 153.30. EI-MS (*m/z*): 311 (M$^+$), 199, 198, 154, 127, 69 (base), 67. HR-MS (EI): M$^+$ found, 311.0974; calcd for C$_{18}$H$_{17}$NO$_2$S, 311.0980.

2-(*N,N*-Dimethylamino)ethyl Carbamate HCl (8). Colorless solid, mp 207–208 °C (lit. mp 212–213 °C[20]); 213–214 °C[22]). IR (Nujol): 1710, 1331, 1219, 1099, 1055, 1033, 760 cm^{-1}. ^{1}H NMR (DMSO-d_6): 2.67 (s, 6H), 3.3–3.4 (overlaps with DMSO signal), 4.51 (t, J ~ 6 Hz, 2H), 7.26–7.30 (m, 2H), 7.36–7.40 (m, 2H), 7.49 (dd, J ~ 7.7 and 2.0 Hz, 2H), 7.74 (broad d, J ~ 8 Hz, 2H), 11.1 (very broad s, 1H). ^{13}C NMR (DMSO-d_6): 42.44, 54.93, 60.94, 126.83, 127.21, 127.31, 127.50, 131.31, 137.67, 152.29. EI-MS (*m/z*): 314 (M$^+$), 243, 200, 199, 198, 172, 167, 166, 154, 127, 116, 72, 58 (base). HR-MS (EI): M$^+$ found, 314.1091; calcd for C$_{17}$H$_{18}$N$_2$O$_2$S, 314.1089.

2-(*N,N*-Diethylamino)ethyl Carbamate HCl (9). Colorless crystals, mp 161–163 °C (lit. mp 163–164 °C[20]). IR (Nujol): 1728, 1712, 1330, 1263, 1219, 1099, 1033, 759 cm^{-1}. ^{1}H NMR (D$_2$O): 0.90 (t, J = 7.2 Hz, 6H), 2.79 (q, J = 7.2 Hz, 4H), 3.11 (broad s, 2H), 4.31 (broad t, $J \approx$ 4,5 Hz, 2H), 6.92–6.95 (m, 2H), 7.02 (broad d, J ~ 7.3 Hz, 2H), 7.10–7.14 (m, 2H), 7.35 (broad d, J ~ 8.1 Hz, 2H). In DMSO-d_6 solution, the N–H signal occurs at 11.13 (broad s, 1H). ^{13}C NMR (D$_2$O): 8.36, 48.49, 50.00, 61.46, 127.23, 127.34, 127.66, 127.69, 131.91, 137.26, 153.70. EI-MS (*m/z*): 342 (M$^+$), 338, 337, 270, 199, 198, 163, 136, 135, 100, 99, 86 (base). HR-MS (EI): M$^+$ found, 342.1405; calcd for C$_{19}$H$_{22}$O$_2$N$_2$S, 342.1402.

3-(*N,N*-Diethylamino)propyl Carbamate HCl (10). Colorless crystals, mp 188–189 °C (lit. mp 195–197 °C[22]). IR (Nujol): 2577, 2490, 1718, 1318, 1286, 1259, 1214, 1045, 1034, 789, 751 cm^{-1}. ^{1}H NMR (D$_2$O): 0.97 (t, J = 7.2 Hz, 6H), 1.68–1.75 (m, 2H), 2.71 (t, J = 8.1 Hz, 2H), 2.83 (t, J = 7.2 Hz, 4H), 4.03–4.09 (m, 2H), 6.87–6.91 (m, 2H), 6.96 (broad d, J ~ 7.7 Hz, 2H), 7.09–7.13 (m, 2H), 7.36 (broad d, J ~ 8.0 Hz, 2H). ^{13}C NMR (D$_2$O): 8.22, 22.43, 47.42, 47.86, 63.78, 126.97, 127.11, 127.41 (2 peaks), 131.60, 137.49, 153.90. EI-MS (*m/z*): 356 (M$^+$ for freebase; base peak), 341, 284, 199, 198, 114, 86. HR-MS (EI): M$^+$ found, 356.1552; calcd for C$_{20}$H$_{24}$N$_2$O$_2$S, 356.1558.

2-(1-Pyrrolidinyl)ethyl carbamate (11). Colorless crystals, mp 61–62 °C (lit. mp of hydrochloride 215–217 °C[20]). IR (Nujol): 1728, 1307, 1261, 1221, 1160, 1053, 755 cm^{-1}. ^{1}H NMR (CDCl$_3$): 1.68–1.77 (m, 4H), 2.46–2.49 (m, 4H), 2.73 (t, J = 6.1 Hz, 2H), 4.33 (t, J = 6.1 Hz, 2H), 7.14–7.18 (m, 2H), 7.25–7.29 (m, 2H), 7.35 (dd, J = 7.8 and 1.2 Hz, 2H), 7.57 (dd, J = 8.1 and 1.0 Hz, 2H). ^{13}C NMR (CDCl$_3$): 23.60, 54.22, 54.50, 65.72, 126.36, 126.78, 127.17, 127.48, 132.24, 138.41, 153.64. EI-MS (*m/z*): 340 (M$^+$), 243, 199, 198, 98, 97 (base), 84. HR-MS (EI): M$^+$ found, 340.1268; calcd for C$_{19}$H$_{20}$N$_2$O$_2$S, 340.1245.

2-(1-Piperidinyl)ethyl Carbamate (12). Colorless crystals, mp 92.2–93.5 °C. IR (Nujol): 1719, 1313, 1287, 1260, 1048, 1036, 984, 756 cm^{-1}. ^{1}H NMR (CDCl$_3$): 1.37–1.43 (m, 2H), 1.51–1.58 (m, 4H), 2.35–2.42 (m, 4H), 2.59 (t, J = 5.9 Hz, 2H), 4.32 (t, J = 5.9 Hz, 2H), 7.14–7.18 (m, 2H), 7.24–7.29 (m, 2H), 7.34 (dd, J = 7.8 and 1.1 Hz, 2H), 7.59 (broad d, J ~ 8.1 Hz, 2H). ^{13}C NMR (CDCl$_3$): 24.24, 26.15, 54.74, 57.25, 64.26, 126.33, 126.75, 127.17, 127.47, 132.19, 138.44, 153.62. EI-MS (*m/z*): 354 (M$^+$), 199, 198, 167, 154, 113, 112 (base), 111, 98. HR-MS (EI): M$^+$ found, 354.1414; calcd for C$_{20}$H$_{22}$N$_2$O$_2$S, 354.1402.

2-(4-Morpholino) Ethyl Carbamate (13). Pale-yellow crystals, mp 99.5–102 °C (lit. mp of hydrochloride 213–214 °C[23]), 218 °C (Szabo et al., 1980[28])). IR (Nujol): 1724, 1324, 1305, 1257, 1224, 1152, 1116, 1056, 758 cm^{-1}. ^{1}H NMR (CDCl$_3$): 2.41–2.45 (m, 4H), 2.61 (t, J = 5.7 Hz, 2H), 3.63–3.68 (m, 4H), 4.33 (t, J = 5.7 Hz, 2H), 7.15–7.19 (m, 2H), 7.25–7.29 (m, 2H), 7.36 (dd, J = 7.7 and 1.3 Hz, 2H), 7.57 (dd, J = 8.1 and 1.0 Hz, 2H). ^{13}C NMR (CDCl$_3$): 53.72, 56.95, 63.75, 67.03, 126.40, 126.73, 127.09, 127.49, 132.22, 138.31, 153.55. EI-MS (*m/z*): 356 (M$^+$), 243, 199, 198, 114 (base), 113, 100. HR-MS (EI): M$^+$ found, 356.1193; calcd for C$_{19}$H$_{20}$N$_2$O$_3$S, 356.1194.

Phenyl Carbamate (14). Colorless crystals, mp 165–166 °C (lit. mp 166 °C[24]). IR (Nujol): 1725, 1589, 1331, 1287, 1267, 1214, 1197, 1126, 1023, 764, 749 cm^{-1}. ^{1}H NMR (CDCl$_3$): 7.16–7.43 (overlapping m, 11H), 7.68 (dd, J = 8.0 and 1.1 Hz, 2H). ^{13}C NMR (CDCl$_3$): 121.43, 125.72, 126.65, 126.91, 126.95, 127.62, 129.31, 132.27, 137.99, 149.92, 150.90. EI-MS (*m/z*): 319 (M$^+$, base), 199, 198, 166, 154, 77. HR-MS (EI): M$^+$ found, 319.0661; calcd for C$_{19}$H$_{13}$O$_2$ NS, 319.0667.

2-Methylphenyl Carbamate (15). Pale-yellow crystals, mp 199–200 °C. IR (Nujol): 1732, 1329, 1228, 1173, 1110, 1012, 944, 766, 753 cm^{-1}. ^{1}H NMR (CDCl$_3$): 2.21 (s, 3H), 7.11–7.26 (overlapping m, 6H), 7.31–7.36 (m, 2H), 7.44 (dd, J = 7.6 and 1.5 Hz, 2H), 7.70 (dd, J = 7.9 and 1.1 Hz, 2H). ^{13}C NMR (CDCl$_3$): 16.52, 122.08, 126.16, 126.95, 127.07, 127.20, 127.36, 127.86, 130.47, 131.30, 132.71, 138.42, 149.76, 152.22. EI-MS (*m/z*): 333 (M$^+$), 201, 199 (base), 171, 167, 154, 127, 91, 77, 65. HR-MS (EI): M$^+$ found, 333.0827; calcd for C$_{20}$H$_{15}$O$_2$NS, 333.0823.

3-Methylphenyl Carbamate (16). Colorless crystals, mp 146–147.5 °C. IR (Nujol): 1722, 1615, 1588, 1333, 1240, 1215, 1142, 1031, 1020, 1000, 770, 762, 748 cm^{-1}. ^{1}H NMR (CDCl$_3$): 2.32 (s, 3H), 6.96–7.03 (overlapping m, 3H), 7.16–7.24, (overlapping m, 3H), 7.27–7.31 (m, 2H), 7.39 (dd, J = 7.8 and 1.5 Hz, 2H), 7.66 (dd, J = 8.0 and 1.2 Hz, 2H). ^{13}C NMR (CDCl$_3$): 21.53, 118.64, 122.31, 126.79, 126.91, 127.22 (2 peaks), 127.88, 129.32, 132.55, 138.35, 139.80, 151.15, 152.52. EI-MS (*m/z*): 333 (M$^+$), 201, 199 (base), 171, 167, 154, 127, 92, 77, 65. HR-MS (EI): M$^+$ found, 333.0820; calcd for C$_{20}$H$_{15}$O$_2$NS, 333.0823.

4-Methylphenyl Carbamate (17). Colorless needles, mp 168–169 °C. IR (Nujol): 1735, 1722, 1508, 1333, 1260, 1221, 1191, 1013, 793, 759 cm^{-1}. ^{1}H NMR (CDCl$_3$): 2.34 (s, 3H), 7.09 (d, J = 8.4 Hz, 2H), 7.17 (d, J = 8.3 Hz, 2H), 7.20–7.23 (m, 2H), 7.30–7.34 (m, 2H), 7.42 (dd, J = 7.8 and 1.0 Hz, 2H), 7.69 (broad d, J ~ 8.0 Hz, 2H). ^{13}C NMR (CDCl$_3$): 20.77, 121.07, 126.57, 126.90 (2 peaks), 127.57, 129.77, 132.24, 135.30, 138.07, 148.71, 152.29. EI-MS (*m/z*): 333 (M$^+$; base), 199, 198, 166, 154, 91. HR-MS (EI): M$^+$ found, 333.0813; calcd for C$_{20}$H$_{15}$O$_2$NS, 333.0823.

2-Methoxyphenyl Carbamate (18). Colorless crystals, mp 156.5–158 °C. IR (Nujol): 1737, 1607, 1586, 1501, 1481, 1330, 1310, 1261, 1209, 1195, 767, 754 cm^{-1}. ^{1}H NMR (CDCl$_3$): 3.92 (s, 3H), 6.90–6.93 (m, 1H), 6.98 (dd, J = 8.3 and 1.2 Hz, 2H), 7.10 (dd, J = 7.9 and 1.6 Hz, 1H), 7.16–7.20 (overlapping m, 3H), 7.27–7.31 (m, 2H), 7.39 (dd, J = 7.8 and 1.2 Hz, 2H), 7.77 (dd, J = 8.1 and 0.9 Hz, 2H). ^{13}C NMR (CDCl$_3$): 56.00, 112.41, 120.72, 123.02, 126.47, 126.75, 126.88, 126.99, 127.49, 132.11, 138.30, 140.17, 151.32, 151.92. EI-MS (*m/z*): 349 (M$^+$), 198, 171, 166, 154, 140, 127, 95, 92, 79, 77 (base). HR-MS (EI): M$^+$ found, 349.0766; calcd for C$_{20}$H$_{15}$NO$_3$S, 349.0772.

3-Methoxyphenyl Carbamate (19). Colorless crystals, mp 107–109 °C. IR (Nujol): 1725, 1611, 1333, 1304, 1290, 1254, 1218, 1143, 1050, 755 cm^{-1}. ^{1}H NMR (CDCl$_3$): 3.76 (s, 3H), 6.74–6.80 (overlapping m, 3H), 7.17–7.21 (m, 2H), 7.22–7.26 (m, 1H), 7.28–7.32 (m, 2H), 7.40 (dd, $J = 7.8$ and 1.2 Hz, 2H), 7.66 (dd, $J = 8.1$ and 0.8 Hz, 2H). ^{13}C NMR (CDCl$_3$): 55.38, 107.34, 111.80, 113.52, 126.63, 126.88, 126.93, 127.60, 129.64, 132.25, 137.97, 151.84, 152.96, 160.39. EI-MS (m/z): 349 (M$^+$; base), 260, 200, 199, 198, 154, 95. HR-MS (EI): M$^+$ found, 349.0777; calcd for C$_{20}$H$_{15}$NO$_3$S, 349.0772.

4-Methoxyphenyl Carbamate (20). Colorless needles, mp 127–128 °C. IR (Nujol): 1717, 1596, 1509, 1332, 1304, 1256, 1213, 1179, 1038, 1011, 804, 759 cm^{-1}. ^{1}H NMR (CDCl$_3$): 3.75 (s, 3H), 6.84–6.87 (m, 2H), 7.07–7.11 (m, 2H), 7.16–7.20 (m, 2H), 7.27–7.31 (m, 2H), 7.39 (dd, $J = 7.9$ and 1.1 Hz, 2H), 7.66 (dd, $J = 8.1$ and 0.9 Hz, 2H). ^{13}C NMR (CDCl$_3$): 55.52, 114.29, 122.21, 126.57, 126.89 (2 peaks), 127.56, 132.21, 138.04, 144.42, 152.46, 157.16. EI-MS(m/z): 349 (M$^+$), 199, 198 (base), 171, 166, 154, 127, 123, 107, 95, 92, 77. HR-MS (EI): M$^+$ found, 349.0773; calcd for C$_{20}$H$_{15}$NO$_3$S, 349.0772.

2-Chlorophenyl Carbamate (21). Colorless crystals, mp 222–224 °C. IR (Nujol): 1737, 1334, 1261, 1221, 1059, 1031, 1007, 945, 757 cm^{-1}. ^{1}H NMR (DMSO-d_6): 7.30–7.34 (overlapping m, 3H), 7.38–7.44 (overlapping m, 3H), 7.48 (dd, $J = 8.1$ and 1.5 Hz, 1H), 7.56–7.58 (overlapping m, 3H), 7.77 (broad d, $J \sim 7.9$ Hz, 2H). ^{13}C NMR (DMSO-d_6): 124.35, 126.08, 127.04, 127.29, 127.53, 127.82 (2 peaks), 128.54, 130.15, 131.62, 137.42, 146.59, 150.46. EI-MS (m/z): 353 (M$^+$), 226, 199, 198, 154. HR-MS (EI): M$^+$ found, 353.0279; calcd for C$_{19}$H$_{12}$NO$_2$SCl, 353.0277.

3-Chlorophenyl Carbamate (22). Colorless crystals, mp 132–133 °C. IR (Nujol): 1727, 1586, 1334, 1260, 1216, 1134, 1090, 1014, 949, 874, 770, 760, 752 cm^{-1}. ^{1}H NMR (CDCl$_3$): 7.08–7.10 (m, 1H), 7.17–7.26 (overlapping m, 5H), 7.29–7.33 (m, 2H), 7.41 (dd, $J = 7.8$ and 1.2 Hz, 2H), 7.64 (broad d, $J \sim 8$ Hz, 2H). ^{13}C NMR (CDCl$_3$): 119.80, 122.06, 125.96, 126.80 (2 peaks), 126.99, 127.66, 129.99, 132.31, 134.53, 137.75, 151.31, 151.62. EI-MS (m/z): 353 (M$^+$; base), 199, 198, 171, 154, 140, 127, 111. HR-MS (EI): M$^+$ found, 353.0282; calcd for C$_{19}$H$_{12}$NO$_2$SCl, 353.0277.

4-Chlorophenyl Carbamate (23). Colorless crystals, mp 179–180 °C. IR (Nujol): 1737, 1330, 1307, 1220, 1132, 1087, 1009, 850, 806, 764, 756 cm^{-1}. ^{1}H NMR (DMSO-d_6): 7.29–7.34 (overlapping m, 4H), 7.39–7.42 (m, 2H), 7.45–7.48 (m, 2H), 7.54 (dd, $J = 7.8$ and 1.3 Hz, 2H), 7.79 (broad d, $J \sim 7.9$ Hz, 2H). ^{13}C NMR (DMSO-d_6): 123.75, 127.06, 127.08, 127.41, 127.70, 129.37, 130.08, 131.40, 137.50, 149.41, 151.09. EI-MS (m/z): 353 (M$^+$), 198, 171, 166, 154, 140, 128, 127, 113, 111 (base), 99, 75. HR-MS (EI): M$^+$ found, 353.0262; calcd for C$_{19}$H$_{12}$NO$_2$SCl, 353.0277.

3-(N,N-Dimethylamino) Phenyl Carbamate (24). Colorless crystals, mp 181–184 °C. IR (Nujol): 1718, 1622, 1510, 1327, 1260, 1213, 1139, 1018, 999, 763, 750 cm^{-1}. ^{1}H NMR (CDCl$_3$): 2.92 (s, 6H), 6.46–6.59 (overlapping m, 3H), 7.18–7.21 (overlapping m, 3H), 7.29–7.32 (m, 2H), 7.40 (dd, $J = 7.8$ and 1.2 Hz, 2H), 7.68 (dd, $J = 8.0$ and 0.9 Hz, 2H). ^{13}C NMR (CDCl$_3$): 40.49, 105.55, 109.02, 109.93, 126.53, 126.92, 126.97, 127.57, 129.52, 132.22, 138.17, 151.67, 152.02, 152.26. EI-MS (m/z): 362 (M$^+$), 298, 263, 261, 200, 199, 198 (base), 197, 171, 166, 154, 140, 137, 127, 120, 86, 84, 69. HR-MS (EI): M$^+$ found, 362.1093; calcd for C$_{21}$H$_{18}$N$_2$O$_2$S, 362.1089.

2-t-Butylphenyl Carbamate (25). Colorless crystals, 134–135 °C. IR (Nujol): 1728, 1327, 1306, 1285, 1261, 1238, 1211, 1186, 1010, 766, 756 cm^{-1}. ^{1}H NMR (CDCl$_3$): 1.16 (s, 9H), 7.18–7.22 (m, 1H), 7.24–7.40 (overlapping, m, 7H), 7.48 (broad d, $J \sim 7.8$ Hz, 2H), 7.74 (broad d, $J \sim 7.9$ Hz, 2H). ^{13}C NMR (CDCl$_3$): 29.95, 34.19, 123.87, 125.58, 126.76, 126.80, 126.98, 127.03, 127.35, 127.54, 132.71, 138.09, 141.33, 149.39, 152.34. EI-MS (m/z): 375 (M$^+$), 200, 199, 198 (base), 91. HR-MS (EI): M$^+$ found, 375.1300; calcd for C$_{23}$H$_{21}$NO$_2$S, 375.1293.

4-t-Butylphenyl Carbamate (26). Colorless crystals, 139.5–140.3 °C. IR (Nujol): 1725, 1512, 1332, 1266, 1215, 1173, 1012, 866, 859, 807, 764, 756 cm^{-1}. ^{1}H NMR (CDCl$_3$): 1.29 (s, 9H), 7.09–7.12 (m, 2H), 7.17–7.21 (m, 2H), 7.27–7.31 (m, 2H), 7.34–7.41 (overlapping m, 4H), 7.67 (broad d, $J \sim 8.0$ Hz, 2H). ^{13}C NMR (CDCl$_3$): 31.37, 34.42, 120.71, 126.20, 126.57, 126.89, 126.92, 127.57, 132.23, 138.10, 148.57, 152.27. EI-MS (m/z): 375 (M$^+$; base), 200, 199, 198, 166, 154. HR-MS (EI): M$^+$ found, 375.1297, calcd for C$_{23}$H$_{21}$NO$_2$S, 375.1293.

4-Biphenyl Carbamate (27). Colorless crystals, 226–227 °C. IR (Nujol): 1731, 1333, 1262, 1219, 1168, 1019, 1006, 760 cm^{-1}. ^{1}H NMR (CDCl$_3$): 7.19–7.33 (m, 2H), 7.24–7.28 (m, 2H), 7.29–7.34 (overlapping m, 3H), 7.39–7.43 (overlapping m, 4H), 7.53–7.58 (overlapping m, 4H), 7.69 (dd, $J = 8.1$ and 0.9 Hz, 2H). ^{13}C NMR (CDCl$_3$): 121.69, 126.70, 126.93, 126.98, 127.08, 127.31, 127.65, 128.05, 128.76, 132.31, 138.02, 138.88, 140.31, 150.36, 152.13. EI-MS (m/z): 395 (M$^+$; base), 200, 199, 198, 170, 166, 154, 152. HR-MS (EI): M$^+$ found, 395.0988, calcd for C$_{25}$H$_{17}$NO$_2$S, 395.0980.

1-Naphthyl Carbamate (28). Colorless crystals, mp 132–133 °C. IR (Nujol): 1720, 1598, 1510, 1322, 1254, 1226, 1208, 1150, 1091, 1043, 1014, 788, 765 cm^{-1}. ^{1}H NMR (CDCl$_3$): 7.18–7.22 (m, 2H), 7.29–7.33 (m, 2H), 7.40–7.48 (overlapping m, 6H), 7.67–7.70 (m, 1H), 7.76 (dd, $J = 8.1$ and 0.9 Hz, 2H), 7.78–7.82 (m, 2H). ^{13}C NMR (CDCl$_3$): 117.85, 121.15, 125.31, 125.91, 126.34, 126.49, 126.81, 126.94, 127.05, 127.12, 127.69, 127.91, 132.53, 134.60, 138.17, 146.87, 152.25. EI-MS (m/z): 369 (M$^+$), 198, 171, 166, 154, 127, 115 (base), 101, 89, 77. HR-MS (EI): M$^+$ found, 369.0831; calcd for C$_{23}$H$_{15}$NO$_2$S, 369.0823.

2-Naphthyl Carbamate (29). Colorless crystals, mp 205.5–206.5 °C. IR (Nujol): 1720, 1333, 1262, 1216, 1151, 1136, 1013, 804, 751 cm^{-1}. ^{1}H NMR (DMSO-d_6): 7.31–7.35 (m, 2H), 7.42–7.59 (overlapping m, 7H), 7.82–7.87 (overlapping m, 3H), 7.91 (broad d, $J \sim 7.9$ Hz, 1H), 7.96 (broad d, $J \sim 7.8$ Hz, 1H), 7.99 (broad d, $J \sim 8.9$ Hz, 1H). ^{13}C NMR (DMSO-d_6): 118.48, 121.44, 125.88, 126.75, 127.08, 127.13, 127.44 (2 peaks), 127.70 (2 peaks), 129.31, 130.99, 131.47, 133.26, 137.66, 148.28, 151.52. EI-MS (m/z): 369 (M$^+$), 198, 154, 127, 115 (base), 101, 89, 77. HR-MS (EI): M$^+$ found, 369.0810; calcd for C$_{23}$H$_{15}$NO$_2$S, 369.0823.

Enzyme Kinetic Studies. The esterase activity of AChE and BuChE was determined by a modification[25] of the Ellman method[26] using a Milton-Roy 1201 UV–visible spectrophotometer (Milton-Roy, Ivyland, PA), set at $\lambda = 412$ nm. Briefly, 1.35 mL of buffered DTNB solution (pH 8.0), 0.05 mL of enzyme (0.04 units of either human recombinant AChE, purified human serum BuChE, or recombinant BuChE in 0.1% aqueous gelatin containing 0.01% sodium azide and 0.05 mL of 50% aqueous acetonitrile or one of the phenothiazine carbamates dissolved in this solvent at 0.5–5 mM, depending on solubility, in a stoppered cuvette of 1 cm path length). After mixing and bringing the absorbance to zero, substrate (acetylthiocholine for AChE and butyrylthiocholine for BuChE) at 0.03 to 0.16 mM, as appropriate, was added to initiate reaction. Assays were carried out at 23 °C over a 1 min period, taking readings every 5 s, after initial 5 s delay. The ΔA/min at 412 nm was converted to velocity as described earlier.[25]

To test for enzyme deactivation over time, loss of enzyme activity was monitored by adding 0.05 mL of 4.8 mM aqueous thiocholine substrate solution in the cuvette after incubation of the enzyme with inhibitor and buffered DTNB for periods of up to 30 min. A zero-time sample was also obtained by adding enzyme last to initiate reaction and the second-order rate constants for enzyme deactivation (k_a values) were determined.[7,27,28] The k_a value was calculated by plotting ln (e_0/e_t)/[I] against time, where e_0 is the enzymatic activity at time zero (without preincubation of enzyme and inhibitor), e_t is the enzymatic activity at time t min of preincubation, and [I] is the molar concentration of inhibitor. The slope of this plot gave the second-order rate constant (k_a value; see Figure 3 as an example).

For study of reversible inhibition of BuChE, an initial experiment at the highest inhibitor concentration, with subsequent 1:10 serial dilutions of each compound were carried out to obtain an enzyme activity–inhibitor concentration profile. Experiments were generally done at least in triplicate and the values averaged.

Lineweaver–Burk plots were generated for reversible inhibitors by using a fixed amount of BuChE (0.04 unit) and varying amounts of substrate (0.03–0.16 mM, final concentration) in the presence

or absence of the inhibitor. The replot of the slopes of the above double reciprocal plots against inhibitor concentration gave the inhibitor constant (K_i) as the intercept on the *x*-axis (see Figure 4 as example).

Calculation of Molecular Parameters. Molecular mechanics calculations were carried out using the MMFF force field in Spartan '06[29] in which the Merck molecular force field (MMFF) was employed, with the keyword "equilibrium conformer", so that the most stable conformer would be selected.

The structure for the graphical abstract was generated using HyperChem program.[32] Briefly, the crystal structure coordinates of BuChE (PDB ID: 1POI) were downloaded from the protein data bank.[33,34] All amino acids were then deleted from the structure except for the residues contained in the active site. Compound **24**, which can be seen in the active site of this figure was optimized separately at the molecular mechanics level using the HyperChem program.[32]

Butterfly angles were determined using Spartan '06.[29] Briefly, two planes were created using three atoms in each of the aromatic rings of the phenothiazine moiety. Once the planes were created, the angle between these planes was calculated, which gave rise to the butterfly angle.

Log *P* calculations were determined using the AlogPS program, which is available online.[30] This method compares the input structure of the compound to a large collection of organic compounds in a database. The compound was built using a template provided by the program. A simplified molecular input line entry system (SMILES) notation was then generated for the compound. The database assessed the compound based on the SMILES notation and a theoretical Log *P* value was determined that statistically best described the molecule compared to the other molecules in the database based on a variety of parameters.

Supporting Information Available: Tables of purity and HPLC chromatograms of all the synthesized compounds. This material is available free of charge via the Internet at http://pubs.acs.org.

References

(1) Silver, A. *The Biology of Cholinesterases*; Elsevier: Amsterdam, 1974.

(2) Giacobini, E. *Butyrylcholinesterase: Its Function and Inhibitors*; Martin Dunitz: London and New York, 2003.

(3) Darvesh, S.; Hopkins, D. A.; Geula, C. Neurobiology of butyrylcholinesterase. *Nat. Rev. Neurosci.* **2003**, *4*, 131–138.

(4) Birks, J. Cholinesterase inhibitors for Alzheimer's disease. Cochrane Database of Systematic Reviews 2006, 1, Art. No. CD005593, DOI: 10.1002/14651858.CD005593.

(5) Kryger, G.; Silman, I.; Sussman, J. L. Three-dimensional structure of a complex of E2020 with acetylcholinesterase from Torpedo californica. *J. Physiol. Paris* **1998**, *92*, 191–194.

(6) Greenblatt, H. M.; Kryger, G.; Lewis, T.; Silman, I.; Sussman, J. L. Structure of acetylcholinesterase complexed with (−)-galanthamine at 2.3 A resolution. *FEBS Lett.* **1999**, *463*, 321–326.

(7) Darvesh, S.; Walsh, R.; Kumar, R.; Caines, A.; Roberts, S.; Magee, D.; Rockwood, K.; Martin, E. Inhibition of human cholinesterases by drugs used to treat Alzheimer disease. *Alzheimer Dis. Assoc. Disord.* **2003**, *17*, 117–126.

(8) Taylor, P. Anticholinesterase agents. In *Goodman & Gilman's The Pharmacological Basis of Therapeutics* 11th ed.; Brunton, L. L., Lazo, J. S., Parker, K. L., Eds.; McGraw-Hill: New York, 2006; pp 201–216..

(9) Weinstock, M.; Razin, M.; Chorev, M.; Enz, A. Pharmacological evaluation of phenyl-carbamates as CNS-selective acetylcholinesterase inhibitors. *J. Neural. Transm.* **1994**, *43*, 219–225.

(10) Greig, N. H.; Pei, X-F.; Soncrant, T.; Ingram, D.; Brossi, A. Phenserine and ring-C hetero-analogues: drug candidates for the treatment of Alzheimer's disease. *Med. Chem. Rev.* **1995**, *15*, 3–31.

(11) Greig, N. H.; Utsuki, T.; Ingram, D. K.; Wang, Y.; Pepeu, G.; Scali, C.; Yu, Q. S.; Mamczarz, J.; Holloway, H. W.; Giordano, T.; Chen, D.; Furukawa, K.; Sambamurti, K.; Brossi, A; Lahiri, D. K. Selective butyrylcholinesterase inhibition elevates brain acetylcholine, augments learning and lowers Alzheimer beta-amyloid peptide in rodent. *Proc. Natl. Acad. Sci. U.S.A.* **2005**, *102*, 17213–17218.

(12) Greig, N. H.; Sambamurti, K.; Yu, Q. S.; Brossi, A.; Bruinsma, G.; Lahiri, D. K. An overview of phenserine tartrate, a novel acetylcholinesterase inhibitor for the treatment of Alzheimer's disease. *Curr. Alzheimer's Res.* **2005**, *2*, 281–291.

(13) Debord, J.; Merle, L.; Bollinger, J. C.; Dantoine, T. Inhibition of butyrylcholinesterase by phenothiazine derivatives. *J. Enzyme Inhib. Med. Chem.* **2002**, *17*, 197–202.

(14) Darvesh, S.; McDonald, R. S.; Penwell, A.; Conrad, S.; Darvesh, K. V.; Mataija, D.; Gomez, G.; Caines, A.; Walsh, R.; Martin, E. Structure–activity relationships for inhibition of human cholinesterases by alkyl amide phenothiazine derivatives. *Bioorg. Med. Chem.* **2005**, *13*, 211–222.

(15) Darvesh, S.; McDonald, R. S.; Darvesh, K. V.; Mataija, D.; Conrad, S.; Gomez, G.; Walsh, R.; Martin, E. Selective reversible inhibition of human butyrylcholinesterase by aromatic amide derivatives of phenothiazine. *Bioorg. Med. Chem.* **2007**, *15*, 6367–6378.

(16) Darvesh, S.; MacKnight, C.; Rockwood, K. Butyrylcholinesterase and cognitive function. *Int. Psychogeriatr.* **2001**, *13*, 461–464.

(17) Saxena, A.; Redman, A. M.; Jiang, X.; Lockridge, O.; Doctor, B. P. Differences in active site gorge dimensions of cholinesterases revealed by binding of inhibitors to human butyrylcholinesterase. *Biochemistry* **1997**, *36*, 14642–14651.

(18) Leszczynski, J. F.; Rose, G. D. Loops in Globular Proteins: A Novel Category of Secondary Structure. *Science.* **1986**, *234*, 849–855.

(19) Velan, B.; Barak, D.; Ariel, N.; Leitner, M.; Bino, T.; Ordentlich, A.; Shafferman, A. Structural modifications of the omega loop in human acetylcholinesterase. *FEBS Lett.* **1996**, *395*, 22–28.

(20) Dahlbom, R. Basically substituted derivatives of 10-phenothiazine carboxylic acid. *Acta Chem. Scand.* **1953**, *7*, 879–884.

(21) Clarke, D.; Gilbert, B. C.; Hanson, P.; Kirk, C. M. Heterocyclic free radicals. Part 8. The influence of the structure and the conformation of the side chain on the properties of phenothiazine cation-radicals substituted at nitrogen. *J. Chem. Soc., Perkin Trans. 2* **1978**, *10*, 1103–1110.

(22) Szabo, W. A.; Chung, R. H.; Tam, C. C.; Tishler, M. Synthetic applications and mechanism of the pyrolysis of phenothiazine carbamates. *J. Org. Chem.* **1980**, *45*, 744–746.

(23) Weston, A. W.; DeNet, R. W.; Michaels, R. J., Jr. Antispasmodics. Basic esters and amides of some heterocyclic *N*-carboxylic acids. *J. Am. Chem. Soc.* **1953**, *75*, 4006–4008.

(24) Stoss, P.; Satzinger, G. Cyclishe sulfoximines, VI. Transannulare acylivanderungen in cyclischen sulfoximiden. *Chem. Ber.* **1978**, *111*, 1453–1463.

(25) Darvesh, S.; Kumar, R.; Roberts, S.; Walsh, R.; Martin, E. Butyrylcholinesterase-mediated enhancement of the enzymatic activity of trypsin. *Cell. Mol. Neurobiol.* **2001**, *21*, 285–296.

(26) Ellman, G. L.; Courtney, K. D.; Andres, V. J.; Featherstone, R. M. A new and rapid colorimetric determination of acetylcholinesterase activity. *Biochem. Pharmacol.* **1961**, *7*, 88–95.

(27) Webb, J. L. *Enzyme and metabolic inhibitors*, Vol *I*.: New York: Academic Press, 1963, 535−603..

(28) Reiner, E.; Radić, Z. Mechanism of action of cholinesterase inhibitors. In *Cholinesterases and Cholinesterase Inhibitors*; Giacobini, E., Ed.; Martin Dunitz Ltd.: London, 2000; pp 103−119..

(29) *Spartan '06*; Wavefunction, Inc.: Irvine, CA, 2006.

(30) Tetko, I. V.; Tanchuk, V. Y.; Villa, A. E. Prediction of *n*-octanol/water partition coefficients from PHYSPROP database using artificial neural networks and E-state indices. *J. Chem. Inf. Comput. Sci.* **2001**, *41*, 1407–1421.

(31) Masson, P.; Legrand, P.; Bartels, C. F.; Froment, M.-T.; Schopfer, L. M.; Lockridge, O. Role of aspartate 70 and tryptophan 82 in binding of succinyldithiocholine to human butyrylcholinesterase. *Biochemistry* **1997**, *36*, 2266–2277.

(32) *HyperChem Release 7.51 for Windows*; Hypercube, Inc.: Gainesville, FL, 2002.

(33) Nicolet, Y.; Lockridge, O.; Masson, P.; Fontecilla-Camps, J. C.; Nachon, F. Crystal structure of human butyrylcholinesterase and of

its complexes with substrate and products. *J. Biol. Chem.* **2003**, *278*, 41141–41147.

(34) Berman, H. M.; Westbrook, J.; Feng, Z.; Gilliland, G.; Bhat, T. N.; Weissig, H.; Shindyalov, I. N.; Bourne, P. E. The Protein Data Bank. *Nucleic Acids Res.* **2000**, *28*, 235, http://www.pdb.org/

(35) DeLano, W. L. *The PyMOL Molecular Graphics System*; DeLano Scientific, San Carlos, CA, 2002; http://www.pymol.org.